Interval Type-2 Fuzzy Logic Modeling and Control of a Mobile Two-Wheeled Inverted Pendulum

Jian Huang , *Senior Member, IEEE*, MyongHyok Ri, Dongrui Wu , *Senior Member, IEEE*, and Songhyok Ri

Abstract—**This paper presents an integrated interval type-2 fuzzy logic approach that simultaneously models and controls an underactuated mobile two-wheeled inverted pendulum (MTWIP), which suffers from modeling uncertainties and external disturbances. The control objective is to attain the desired position and direction while keeping the MTWIP balanced. It is achieved by integrating four interval type-2 fuzzy logic systems (IT2 FLSs): the first IT2 FLS describes the dynamics of the MTWIP using a Takagi–Sugeno model, the second IT2 FLS controls the balance of the MTWIP using also a Takagi–Sugeno model, and the third and fourth IT2 FLSs control its position and direction, respectively, using a Mamdani model. A linear matrix inequality based design approach is also proposed to guarantee the stability of the balance controller. The proposed approach is compared with a type-1 FLS in real-world experiments. All results demonstrate that the IT2 FLS outperforms the type-1 FLS, especially under modeling uncertainties and external disturbances.**

Index Terms—**Balance control, interval type-2 (IT2) fuzzy logic control, linear matrix inequality (LMI), mobile two-wheeled invert pendulum.**

I. INTRODUCTION

THE inverted pendulum has widely established itself in the literature and practice as a platform for demonstrating various control strategies. Recently, the mobile two-wheeled inverted pendulum (MTWIP) has gained increasing interest [1], [8]–[11], [15], [16], [21], [22], [33]–[35], because its nonlinear multiple-input multiple-output characteristics enables the demonstration of more sophisticated control approaches, and also because it has been widely used in our everyday life (e.g., self-balancing scooters from Ninebot/Segway and many other companies). For example, Pathak *et al.* [33] analyzed the dynamics of the MTWIP and controlled its velocity and position using partial feedback linearization. Huang *et al.* [15] proposed a dynamic model of an underactuated MTWIP-based narrow vehicle (called UW-Car) and then designed two terminal sliding mode controllers to control its velocity and braking. Ri *et al.* [34] designed a nonlinear disturbance observer for the MTWIP system in order to eliminate the main drawback of sliding mode control, the "chattering" phenomenon, and to compensate the model uncertainties and external disturbances.

Fuzzy logic systems (FLSs), which have been used in a broad range of applications, have also found applications on MTWIPs [14], [30], [46]. For example, Huang *et al.* [14] designed a type-1 (T1) FLS for an MTWIP using the Takagi–Sugeno (TS) model and Mamdani inference. Xu *et al.* [46] proposed a novel implementation of a T1 TS FLS for an MTWIP using full-state feedback. In both approaches, the control objective was to achieve position control of the MTWIP while keeping it balanced. Generally, the dynamics of the MTWIP can be represented by a TS fuzzy model, and then a parallel distributed compensation FLS can be designed using linear matrix inequality (LMI) approaches, with guaranteed stability [20], [38].

Recently it has been shown that interval type-2 fuzzy sets (IT2 FSs) [27], [28], an extension of T1 FSs, are better able to model and cope with uncertainties, as demonstrated by a number of applications [6], [12], [23]–[27], [36], [36], [37], [39], [42]–[44], including the modeling and control of mobile inverted pendulums [3], [7], [29]. For example, Mohammad *et al.* [29] designed an IT2 fuzzy PID controller using a new type-reduction method to control an inverted pendulum on a cart system with an uncertain model. Benjamas and Ahmad [3] proposed an IT2 TS FLS for the balancing and position control of a wheelchair.

However, most existing FLSs for mobile-inverted pendulums only considered balance control. Other important considerations, including position control and direction control, have not been paid enough attention. Furthermore, to our best knowledge, IT2 FLSs have not been applied to the position and direction control of MTWIPs. This problem is investigated in this paper. Our main contributions are:

1) We propose the first integrated IT2 FLS approach that models the uncertain dynamics of an MTWIP, and controls its balance, position, and direction simultaneously.
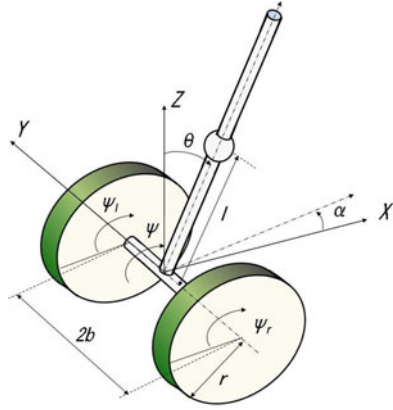
Fig. 1.   MTWIP system.

2) We introduce an LMI-based approach to guarantee the stability of the balance controller.
3) We demonstrate the superior performance of the proposed IT2 FLS in real-world experiments.

The rest of this paper is organized as follows. Section II presents the dynamic model and the equivalent TS fuzzy model of the MTWIP, considering both modeling uncertainties and external disturbances. Section III introduces the IT2 FLSs for controlling the balance, position, and direction of the MTWIP, and also the LMI-based stability analysis of the balance controller. Section IV presents real-world experimental results to verify the effectiveness and robustness of the proposed approach by comparing it with a T1 FLS. Section V discusses the robustness and stability of the proposed IT2 FLS. Finally, Section VI draws conclusions.

Notations: Throughout this paper, we use capital letters to denote matrices, lower case letters to denote scalars, bold lower case letters to denote vectors, $\dot{x}$ to denote the first order derivative of x, $\ddot{x}$ to denote the second-order derivative of x, $\hat{x}$ to denote the measured value of x, and $\tilde{X}$ to denote an IT2 FS.

II. Dynamics and IT2 TS Fuzzy Modeling of the MTWIP

Fig. 1 illustrates the MTWIP system [16], where r is radius of the wheel, and ψ_l and ψ_r are the rotation angles of the left and right wheels, respectively. $2b$ is the distance between the two wheels. l is the distance between the wheel axle and the center of the gravity of the inverted pendulum. α is the yaw angle of the MTWIP, and θ is the inclination angle of the inverted pendulum.

The dynamic model of the MTWIP system can be expressed by [15]

$$
\begin{cases}
\hat{m}_{11}\ddot{\psi} + \hat{m}_{12}\ddot{\theta}\cos\theta = \hat{m}_{12}(\dot{\theta}^2 + \dot{\alpha}^2)\sin\theta \\
\quad -2\hat{d}_w\dot{\psi} + 2\hat{d}_b(\dot{\theta} - \dot{\psi}) + u_r + u_l + \hat{\tau}_1 \\
\hat{m}_{12}\ddot{\psi}\cos\theta + \hat{m}_{22}\ddot{\theta} = \hat{n}_{bla}\dot{\alpha}^2\sin\theta\cos\theta \\
\quad +\hat{g}_b\sin\theta - 2\hat{d}_b(\dot{\theta} - \dot{\psi}) - u_r - u_l + \hat{\tau}_2 \\
(\hat{n}_{bla}\sin^2\theta + \hat{m}_{33})\ddot{\alpha} = -2\hat{n}_{bla}\dot{\alpha}\dot{\theta}\sin\theta\cos\theta \\
\quad -\hat{m}_{12}\dot{\alpha}\dot{\psi}\sin\theta - \frac{2\hat{b}^2}{\hat{r}^2}(\hat{d}_b + \hat{d}_w)\dot{\alpha} + \frac{\hat{b}}{\hat{r}}(u_r - u_l) + \hat{\tau}_3
\end{cases}
\tag{1}
$$

where

$$
\begin{cases}
\psi &= \frac{1}{2}(\psi_r + \psi_l) \\
\hat{m}_{11} &= (\hat{m}_b + 2\hat{m}_w)\hat{r}^2 + 2\hat{n}_{wa} \\
\hat{m}_{12} &= \hat{m}_b\hat{l}\hat{r} \\
\hat{m}_{22} &= \hat{m}_b\hat{l}^2 + \hat{n}_{yb} \\
\hat{n}_{bla} &= \hat{n}_{zb} + \hat{m}_b\hat{l}^2 \\
\hat{g}_b &= \hat{m}_b g\hat{l} \\
\hat{m}_{33} &= 2\hat{n}_{wd} + \frac{2\hat{b}^2}{\hat{r}^2}(\hat{n}_{wa} + \hat{m}_w\hat{r}^2)
\end{cases}
$$

in which m_b and m_w are the masses of the pendulum body and a wheel, respectively; n_{yb} and n_{zb} are the moments of the inertia of the body about the *Y*-axis and *Z*-axis, respectively; n_{wa} and n_{wd} are the moments of inertia of a wheel about its axis and a diameter; d_b and d_w are the resistances in the driving system and ground, respectively; u_l and u_r are rotation torques generated by the left and right motors coaxial with the wheels, respectively; and $\hat{\tau}_i$ $(i = 1, 2, 3)$ denotes the combination of measurement uncertainties and external disturbances of the system.

The control objective is to balance the MTWIP and to simultaneously control its movement position and direction. For balance control, only the first two equations in (1) are needed. We can rewrite them as

$$
\begin{bmatrix} \hat{m}_{12}\cos\theta & \hat{m}_{11} \\ \hat{m}_{22} & \hat{m}_{12}\cos\theta \end{bmatrix} \begin{bmatrix} \ddot{\theta} \\ \ddot{\psi} \end{bmatrix} =
$$

$$
\begin{bmatrix} \hat{m}_{12}(\dot{\theta}^2 + \dot{\alpha}^2)\sin\theta - 2\hat{d}_w\dot{\psi} + 2\hat{d}_b(\dot{\theta} - \dot{\psi}) + u_r + u_l + \hat{\tau}_1 \\ \hat{n}_{bla}\dot{\alpha}^2\sin\theta\cos\theta + \hat{g}_b\sin\theta - 2\hat{d}_b(\dot{\theta} - \dot{\psi}) - u_r - u_l + \hat{\tau}_2 \end{bmatrix}
$$

which is equivalent to

$$
\begin{bmatrix} \ddot{\theta} \\ \ddot{\psi} \end{bmatrix} = \frac{1}{\Delta} \begin{bmatrix} \hat{m}_{12}\cos\theta & -\hat{m}_{11} \\ -\hat{m}_{22} & \hat{m}_{12}\cos\theta \end{bmatrix} \cdot
$$

$$
\begin{bmatrix} \hat{m}_{12}(\dot{\theta}^2 + \dot{\alpha}^2)\sin\theta - 2\hat{d}_w\dot{\psi} + 2\hat{d}_b(\dot{\theta} - \dot{\psi}) + u_r + u_l + \hat{\tau}_1 \\ \hat{n}_{bla}\dot{\alpha}^2\sin\theta\cos\theta + \hat{g}_b\sin\theta - 2\hat{d}_b(\dot{\theta} - \dot{\psi}) - u_r - u_l + \hat{\tau}_2 \end{bmatrix}
\tag{2}
$$

where $\Delta = \hat{m}_{12}^2\cos^2\theta - \hat{m}_{11}\hat{m}_{22}$.

Note that the terms including yaw angle α and its derivatives can be viewed as the disturbances in balance control. Choose the state vector as $\mathbf{x} = [x_1, \ x_2, \ x_3, \ x_4]^T = [\theta, \ \dot{\theta}, \ \psi, \ \dot{\psi}]^T$, where the inclination angle $\theta \in [-\frac{\pi}{6}, \ \frac{\pi}{6}]$. The state model of the disturbance-free model (2) is

$$
\dot{\mathbf{x}} = \mathbf{f}(\mathbf{x}) + \mathbf{g}(\mathbf{x})u
\tag{3}
$$

where

$$
\mathbf{f}(\mathbf{x}) = \frac{1}{\Delta}[f_1, f_2, f_3, f_4]^T
$$

$$
\mathbf{g}(\mathbf{x}) = \frac{1}{\Delta} \begin{bmatrix} \hat{m}_{11} + \hat{m}_{12}\cos x_1 \\ -\hat{m}_{22} - \hat{m}_{12}\cos x_1 \end{bmatrix}
$$

and u is the input of the system. Here f_i $(i = 1, 2, 3, 4)$ satisfy

$$
\begin{cases}
f_1 = \Delta \cdot x_2 \\
f_2 = \hat{m}_{12}^2 x_2^2 \cos x_1 \sin x_1 - 2\hat{m}_{12} \cos x_1 \hat{d}_w x_4 \\
\quad\quad - \hat{m}_{11} \hat{g}_b \sin x_1 + 2\hat{m}_{12} \cos x_1 \hat{d}_b (x_2 - x_4) \\
\quad\quad + 2\hat{m}_{11} \hat{d}_b (x_2 - x_4) \\
f_3 = \Delta \cdot x_4 \\
f_4 = -\hat{m}_{22} \hat{m}_{12} x_2^2 \sin x_1 + 2\hat{m}_{22} \hat{d}_w x_4 \\
\quad\quad - 2\hat{m}_{22} \hat{d}_b (x_2 - x_4) + \hat{m}_{12} \hat{g}_b \cos x_1 \sin x_1 \\
\quad\quad - 2\hat{m}_{12} \hat{d}_b (x_2 - x_4) \cos x_1.
\end{cases}
$$

Using local approximation in fuzzy partition spaces, a TS fuzzy model can be derived from (3). When x_1 is close to 0, (3) can be simplified as (4), where $\Delta_1 = \hat{m}_{11}\hat{m}_{22} - \hat{m}_{12}^2$. When x_1 is close to $\pm\frac{\pi}{6}$, (3) can be simplified as (5), where $\Delta_\beta = \hat{m}_{11}\hat{m}_{22} - \hat{m}_{12}^2 \beta_1^2$ and $\beta_1 = \cos\frac{\pi}{6}$. Note that (4) and (5) are now linear systems, (4) as shown bottom of this page.

The linearized models of the MTWIP at $\theta = -\frac{\pi}{6}$ and $\theta = \frac{\pi}{6}$ are identical, so we only need to develop TS fuzzy rules for $\theta = 0$ and $\theta = \frac{\pi}{6}$, and then interpret the dynamics for other inclination angles between them using fuzzy inference. More specifically, the following two rules are enough to describe the dynamics of the MTWIP, (5) as shown bottom of this page.

Model Rule i : If θ is $\tilde{M}_i$, then $\dot{x} = A_i x + B_i u.$ $\quad i = 1, 2$

where $\tilde{M}_i$ is an IT2 FS of Rule i in the domain of θ, and A_i and B_i are the system matrices:

$$
A_1 = \begin{bmatrix}
0 & 1 & 0 & 0 \\
\frac{\hat{m}_{11}\hat{g}_b}{\Delta_1} & -\frac{2\hat{m}_{s1}\hat{d}_b}{\Delta_1} & 0 & \frac{2(\hat{m}_{12}\hat{d}_w + \hat{d}_b \hat{m}_{s1})}{\Delta_1} \\
0 & 0 & 0 & 1 \\
-\frac{\hat{m}_{12}\hat{g}_b}{\Delta_1} & \frac{2\hat{d}_b \hat{m}_{s2}}{\Delta_1} & 0 & -\frac{2(\hat{m}_{22}\hat{d}_w + \hat{d}_b \hat{m}_{s2})}{\Delta_1}
\end{bmatrix}
$$
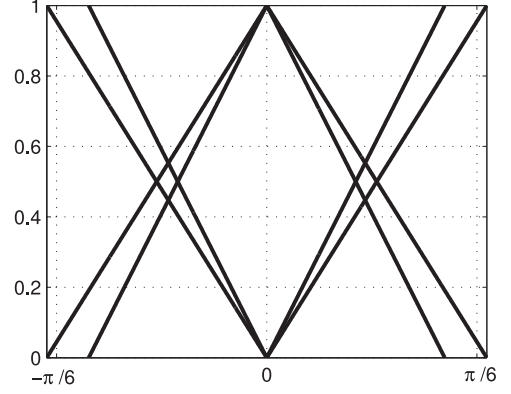
Fig. 2. IT2 FSs for the antecedents of the IT2 TS fuzzy model.

$$
A_2 = \begin{bmatrix}
0 & 1 & 0 & 0 \\
\frac{\hat{m}_{11}\hat{g}_b \beta_1}{\Delta_\beta} & -\frac{2\hat{m}_{\beta1}\hat{d}_b}{\Delta_\beta} & 0 & \frac{2(\hat{m}_{12}\hat{d}_w \beta_1 + \hat{d}_b \hat{m}_{\beta1})}{\Delta_\beta} \\
0 & 0 & 0 & 1 \\
-\frac{\hat{m}_{12}\hat{g}_b \beta_1^2}{\Delta_\beta} & \frac{2\hat{d}_b \hat{m}_{\beta2}}{\Delta_\beta} & 0 & -\frac{2(\hat{m}_{22}\hat{d}_w + \hat{d}_b \hat{m}_{\beta2})}{\Delta_\beta}
\end{bmatrix}
$$

$$
B_1 = \begin{bmatrix} 0 \\ -\frac{(\hat{m}_{11} + \hat{m}_{12})}{\Delta_1} \\ 0 \\ \frac{\hat{m}_{12} + \hat{m}_{22}}{\Delta_1} \end{bmatrix}, \quad
B_2 = \begin{bmatrix} 0 \\ -\frac{(\hat{m}_{12}\beta_1 + \hat{m}_{11})}{\Delta_\beta} \\ 0 \\ \frac{(\hat{m}_{12}\beta_1 + \hat{m}_{22})}{\Delta_\beta} \end{bmatrix}
$$

in which $\hat{m}_{s1} = \hat{m}_{11} + \hat{m}_{12}$, $\hat{m}_{s2} = \hat{m}_{12} + \hat{m}_{22}$, $\hat{m}_{\beta1} = \hat{m}_{11} + \hat{m}_{12}\beta_1$, and $\hat{m}_{\beta2} = \hat{m}_{12}\beta_1 + \hat{m}_{22}$. Triangular IT2 FSs are used as membership functions of $\tilde{M}_i$, as shown in Fig. 2:

$$
\underline{\mu}_{\tilde{M}_1}(\theta) = \begin{cases} \frac{\theta + \pi/7}{\pi/7}, & \theta < 0 \\ 1, & \theta = 0 \\ \frac{\pi/7 - \theta}{\pi/7}, & \theta > 0 \end{cases}, \quad \underline{\mu}_{\tilde{M}_2}(\theta) = 1 - \underline{\mu}_{\tilde{M}_1}(\theta)
$$

$$
\bar{\mu}_{\tilde{M}_1}(\theta) = \begin{cases} \frac{\theta + \pi/6}{\pi/6}, & \theta < 0 \\ 1, & \theta = 0 \\ \frac{\pi/6 - \theta}{\pi/6}, & \theta > 0 \end{cases}, \quad \bar{\mu}_{\tilde{M}_2}(\theta) = 1 - \bar{\mu}_{\tilde{M}_1}(\theta)
$$

$$
\dot{x} = \begin{bmatrix}
x_2 \\
\frac{1}{\Delta_1}\left(\hat{m}_{11}\hat{g}_b x_1 - 2\hat{d}_b(\hat{m}_{12} + \hat{m}_{11})x_2 + 2(\hat{m}_{12}\hat{d}_w + \hat{m}_{11}\hat{d}_b + \hat{m}_{12}\hat{d}_b)x_4\right) \\
x_4 \\
\frac{1}{\Delta_1}\left(-\hat{m}_{12}\hat{g}_b x_1 + 2(\hat{m}_{22}\hat{d}_b + \hat{m}_{12}\hat{d}_b)x_2 - 2(\hat{m}_{22}\hat{d}_w + \hat{m}_{22}\hat{d}_b + \hat{m}_{12}\hat{d}_b)x_4\right)
\end{bmatrix} + \frac{1}{\Delta_1}\begin{bmatrix} -\hat{m}_{11} - \hat{m}_{12} \\ \hat{m}_{22} + \hat{m}_{12} \end{bmatrix} u. \quad (4)
$$

$$
\dot{x} = \begin{bmatrix}
x_2 \\
\frac{1}{\Delta_\beta}\left((\hat{m}_{11}\hat{g}_b \cos\frac{\pi}{6})x_1 - 2\hat{d}_b(\hat{m}_{11} + \hat{m}_{12}\cos\frac{\pi}{6})x_2 + 2(\hat{m}_{12}\hat{d}_w \cos\frac{\pi}{6} + \hat{m}_{11}\hat{d}_b + \hat{m}_{12}\hat{d}_b \cos\frac{\pi}{6})x_4\right) \\
x_4 \\
\frac{1}{\Delta_\beta}\left((-\hat{m}_{12}\hat{g}_b(\cos\frac{\pi}{6})^2)x_1 + 2(\hat{m}_{22}\hat{d}_b + \hat{m}_{12}\hat{d}_b \cos\frac{\pi}{6})x_2 - 2(\hat{m}_{22}\hat{d}_w + \hat{m}_{22}\hat{d}_b + \hat{m}_{12}\hat{d}_b \cos\frac{\pi}{6})x_4\right)
\end{bmatrix}
$$
$$
+ \frac{1}{\Delta_\beta}\begin{bmatrix} -\hat{m}_{11} - \hat{m}_{12}\cos\frac{\pi}{6} \\ \hat{m}_{22} + \hat{m}_{12}\cos\frac{\pi}{6} \end{bmatrix} u \quad (5)
$$

in which $\underline{\mu}_{\tilde{M}_i}(\theta)$ and $\bar{\mu}_{\tilde{M}_i}(\theta)$ are the lower and upper membership functions, respectively. Note that we make $\underline{\mu}_{\tilde{M}_1}(\theta)$ and $\bar{\mu}_{\tilde{M}_2}(\theta)$ complementary to each other to simplify the computation and also the stability analysis.

The firing strength of the ith rule is

$$M_i = \left[\underline{\mu}_{\tilde{M}_i}(\theta),\ \bar{\mu}_{\tilde{M}_i}(\theta) \right], \qquad i = 1, 2.$$

Therefore, the defuzzified output of the IT2 TS fuzzy model, using the Nie–Tan method [31], [40], is

$$
\begin{aligned}
\dot{\mathbf{x}} &= \sum_{i=1}^{2} \frac{\left[\underline{\mu}_{\tilde{M}_i}(\theta) + \bar{\mu}_{\tilde{M}_i}(\theta) \right]/2}{\sum_{j=1}^{2} \left[\underline{\mu}_{\tilde{M}_j}(\theta) + \bar{\mu}_{\tilde{M}_j}(\theta) \right]/2} (A_i \mathbf{x} + B_i u) \\
&= \sum_{i=1}^{2} \frac{\underline{\mu}_{\tilde{M}_i}(\theta) + \bar{\mu}_{\tilde{M}_i}(\theta)}{2} (A_i \mathbf{x} + B_i u) \\
&\equiv \sum_{i=1}^{2} m_i(\theta) (A_i \mathbf{x} + B_i u) \quad (6)
\end{aligned}
$$

where

$$m_i(\theta) = \frac{\underline{\mu}_{\tilde{M}_i}(\theta) + \bar{\mu}_{\tilde{M}_i}(\theta)}{2}.$$

Equation (6) will be considered as the model to be controlled in the next section.

III. IT2 FLSs FOR CONTROLLING THE BALANCE, POSITION, AND DIRECTION OF THE MTWIP

This section introduces the IT2 FLSs for controlling the balance, position, and direction of the MTWIP.

A. Balance Control

Let the desired state of the MTWIP be $\mathbf{x}_d = \left[\theta_d,\ \dot{\theta}_d,\ \psi_d,\ \dot{\psi}_d \right]^T$. The first control objective is to guarantee the balance of the MTWIP by determining the feedback gains G_i, so that the IT2 FLS can drive $\mathbf{x} \to \mathbf{0}$. An IT2 parallel distributed compensation FLS with two rules in the following form is proposed:

Balance Control Rule i : If θ is $\tilde{M}_i$

$$\text{then } u = G_i \mathbf{x}. \quad i = 1, 2$$

where $\tilde{M}_i$ are IT2 FSs defined in Fig. 2, and G_i are the constant local feedback gains to be determined. The defuzzified output, using again the Nie–Tan method, is:

$$
\begin{aligned}
u &= \sum_{i=1}^{2} \frac{\left[\underline{\mu}_{\tilde{M}_i}(\theta) + \bar{\mu}_{\tilde{M}_i}(\theta) \right]/2}{\sum_{j=1}^{2} \left[\underline{\mu}_{\tilde{M}_j}(\theta) + \bar{\mu}_{\tilde{M}_j}(\theta) \right]/2} G_i \mathbf{x} \\
&= \sum_{i=1}^{2} \frac{\underline{\mu}_{\tilde{M}_i}(\theta) + \bar{\mu}_{\tilde{M}_i}(\theta)}{2} G_i \mathbf{x} \equiv \sum_{i=1}^{2} m_i(\theta) G_i \mathbf{x}. \quad (7)
\end{aligned}
$$

The local feedback gains G_i are determined so that the state $\mathbf{x}$ approaches zero asymptotically. Substituting (7) into (6), it follows that:

$$
\begin{aligned}
\dot{\mathbf{x}} &= \sum_{i=1}^{2} m_i(\theta) \left[A_i \mathbf{x} + B_i \sum_{j=1}^{2} m_j G_j \mathbf{x} \right] \\
&= \sum_{i=1}^{2} m_i(\theta) \left[\sum_{j=1}^{2} m_j(\theta) A_i \mathbf{x} + \sum_{j=1}^{2} m_j B_i G_j \mathbf{x} \right] \\
&= \sum_{i=1}^{2} \sum_{j=1}^{2} m_i(\theta) m_j(\theta) (A_i + B_i G_j) \mathbf{x} \\
&= \sum_{i=1}^{2} \sum_{j=1}^{2} m_i(\theta) m_j(\theta) K_{ij} \mathbf{x} \quad (8)
\end{aligned}
$$

where $K_{ij} = A_i + B_i G_j$, and we have used the fact that $m_1(\theta) + m_2(\theta) = 1$.

An LMI-based stability condition guaranteeing the stability of (8) is given by the following lemmas.

Lemma 1: The equilibrium of the FLS in (6) is quadratically stable in the large if there exist symmetric matrices P and W such that

$$
\left.
\begin{aligned}
P &> 0 \\
K_{ii}^T P + P K_{ii} + W_{ii} &< 0 \\
K_{ij}^T P + P K_{ij} + W_{ij} &\le 0 \\
W &= \begin{bmatrix} W_{11} & W_{12} \\ W_{12} & W_{22} \end{bmatrix} > 0
\end{aligned}
\right\} . \quad \square \quad (9)
$$

Proof: Similar to Theorem 7 in [20], choose the Lyapunov function candidate as $V(\mathbf{x}) = \mathbf{x}^T P \mathbf{x}$. The time derivative of $V(\mathbf{x})$ along the solution trajectory is

$$
\begin{aligned}
\dot{V}(\mathbf{x}) &= \dot{\mathbf{x}}^T P \mathbf{x} + \mathbf{x}^T P \dot{\mathbf{x}} \\
&= \sum_{i=1}^{2} m_i^2 \left[\mathbf{x}^T \left(K_{ii}^T P + P K_{ii} \right) \mathbf{x} \right] \\
&\quad + \sum_{i \ne j} m_i m_j \left[\mathbf{x}^T \left(K_{ij}^T P + P K_{ij} \right) \mathbf{x} \right].
\end{aligned}
$$

From (9) we have

$$
\begin{aligned}
K_{ii}^T P + P K_{ii} &< -W_{ii} \\
K_{ij}^T P + P K_{ij} &< -W_{ij}
\end{aligned}
$$

and hence

$$
\begin{aligned}
\dot{V}(\mathbf{x}) &\le -\sum_{i=1}^{2} m_i^2 \mathbf{x}^T W_{ii} \mathbf{x} - \sum_{i \ne j} m_i m_j \mathbf{x}^T W_{ij} \mathbf{x} \\
&= -\begin{bmatrix} m_1 \mathbf{x} \\ m_2 \mathbf{x} \end{bmatrix}^T \begin{bmatrix} W_{11} & W_{12} \\ W_{21} & W_{22} \end{bmatrix} \begin{bmatrix} m_1 \mathbf{x} \\ m_2 \mathbf{x} \end{bmatrix} < 0
\end{aligned}
$$

i.e., $\dot{V}(\mathbf{x})$ is negative definite so that the equilibrium of the FLS in (6) is quadratically stable in the large. ∎

Because $K_{ij} = A_i + B_i G_j$, (9) cannot be solved by the standard LMI. Let

$$Q = P^{-1} \tag{10}$$

$$G_i = -N_i Q^{-1} \tag{11}$$

$$Y_{ij} = Q W_{ij} Q. \tag{12}$$

Then premultiply and postmultiply (8)–(9) by Q, we can obtain:

$$\left. \begin{array}{c} Q > 0 \\ QA_i^T + A_i Q - N_i^T B_i^T - B_i N_i + Y_{ii} < 0 \\ QA_i^T + A_i Q - N_j^T B_i^T - B_i N_j + Y_{ij} < 0 \end{array} \right\}. \tag{13}$$

Note that the inequalities in (13) are LMIs of variables Q, N_i, and Y_{ij}, from which the controller gains G_i can be easily solved.

Lemma 2: For the FLS in (8), suppose the unknown initial state vector $\mathbf{x}_0$ is upper bounded by ε, i.e., $\|\mathbf{x}_0\| \le \varepsilon$. Then, the control input u satisfies $|u| \le \rho$ if the following conditions are added to those in Lemma 1:

$$\left. \begin{array}{c} \varepsilon^2 I \le Q \\ \begin{bmatrix} Q & N_i^T \\ N_i & \rho^2 I \end{bmatrix} \ge 0 \end{array} \right\} \tag{14}$$

where ε and ρ are predefined positive scalars. □

Proof: From (10) and (14) we have

$$P = Q^{-1} \le \frac{1}{\epsilon^2} I \tag{15}$$

and hence

$$\mathbf{x}_0^T P \mathbf{x}_0 \le \frac{1}{\epsilon^2} \mathbf{x}_0^T \mathbf{x}_0 \le 1. \tag{16}$$

According to the Schur complement procedure, LMI (13) is equivalent to

$$\frac{1}{\rho^2} N_i^T N_i - Q \le 0. \tag{17}$$

Since $G_i = -N_i Q^{-1}$, (17) can be rewritten as

$$\frac{1}{\rho^2} G_i^T G_i - Q^{-1} \le 0. \tag{18}$$

From (7) and (18) it follows that

$$\|u\|^2 = u^T u = \sum_{i=1}^{2} \sum_{j=1}^{2} m_i m_j \mathbf{x}^T G_i^T G_j \mathbf{x}$$

$$\le \frac{1}{2} \sum_{i=1}^{2} \sum_{j=1}^{2} m_i m_j \mathbf{x}^T (G_i^T G_i + G_j^T G_j) \mathbf{x}$$

$$\le \rho^2 \sum_{i=1}^{2} \sum_{j=1}^{2} m_i m_j \mathbf{x}^T Q^{-1} \mathbf{x}. \tag{19}$$

Considering the fact that $m_i(\theta) + m_j(\theta) = 1$ and $\dot{V}(\mathbf{x})$ is negative definite, (19) leads to

$$\|u\|^2 \le \rho^2 \mathbf{x}^T Q^{-1} \mathbf{x} = \rho^2 \mathbf{x}^T P \mathbf{x} \le \rho^2.$$

This completes the proof. ∎
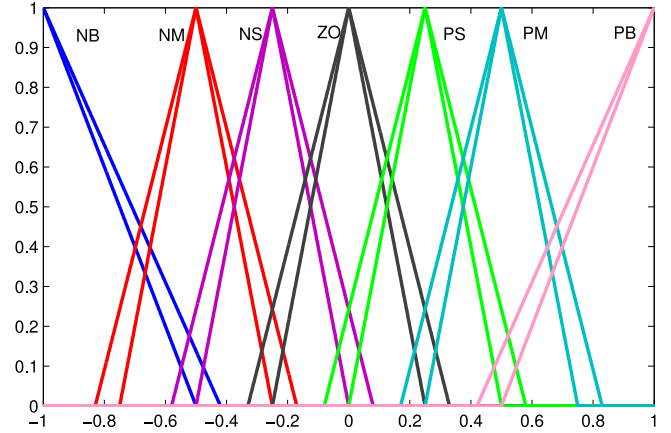
Fig. 3.   IT2 membership functions of the antecedents and consequent in the position and direction controllers.

Based on Lemmas 1 and 2, the control gains G_i can be computed to guarantee $\lim_{t\to\infty} \mathbf{x} = \mathbf{0}$.

B. Position and Direction Control

So far we have introduced the balance controller. Next we will propose two IT2 Mamdani FLSs for the position and direction control of the MTWIP.

Intuitively, when the inverted pendulum leans forward ($\theta > 0$), the MTWIP should also move forward to balance it, and vice versa. So, position control can be achieved by giving a certain inclination angle to the inverted pendulum. Meanwhile, direction control can be achieved by applying the following control signals to the left and right wheels:

$$u_l = u_p - u_\alpha$$

$$u_r = u_p + u_\alpha$$

where u_l and u_r are control signals for the left and right wheels, respectively, u_p is the output of the IT2 position controller, and u_α is the output of the IT2 direction controller.

The position controller employs IT2 Mamdani If–Then rules in the following form:

Position Control Rule i : If p_e is $\tilde{A}_D$ and $\dot{\theta}$ is $\tilde{B}_{\dot{\theta}}$,

Then θ_{off} is $\tilde{C}_D$

where p_e is the error of the position, and $\dot{\theta}$ is the change rate of the inclination angle. Note that the output of the position controller is θ_{off} instead of a direct control signal. As shown in Fig. 4, θ_{off} is then fed into the balance controller. If θ_{off} is not zero, then the balance controller thinks the MTWIP is out of balance, so it drives the MTWIP forward or backward to balance it, but in fact achieves our desired position control.

Similarly, the direction controller employs the following IT2 Mamdani If–Then rules:

Direction Control Rule i : If α_e is $\tilde{A}_\alpha$ and $\dot{\alpha}_e$ is $\tilde{B}_\alpha$

Then u_α is $\tilde{C}_\alpha$
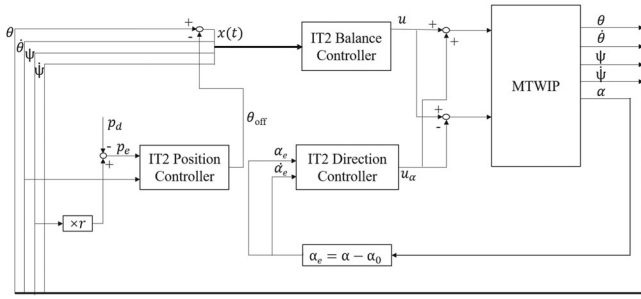
Fig. 4. Overall control diagram for the MTWIP.

Fig. 5. MTWIP in real-world experiments.

TABLE I
RANGES OF THE INPUT AND OUTPUT VARIABLES

Variable	p_e (m)	$\dot{\theta}_e$ (rad/s)	α_e (rad)	$\dot{\alpha}_e$ (rad/s)	θ_{off} (rad)	u_α
Range	$[-3, 3]$	$[-4, 4]$	$[-1, 1]$	$[-1, 1]$	$[-\pi/40, \pi/40]$	$[-200, 200]$

TABLE II
FUZZY RULES FOR POSITION AND DIRECTION CONTROL

$p_e(\alpha_e)$ / $\dot{\theta}_e(\dot{\alpha}_e)$	NB	NM	NS	ZO	PS	PM	PB
NB	PB	PB	PB	PB	PM	PS	ZO
NM	PB	PB	PB	PM	PS	ZO	NS
NS	PB	PB	PM	PS	ZO	NS	NM
ZO	PB	PM	PS	ZO	NS	NM	NB
PS	PM	PS	ZO	NS	NM	NB	NB
PM	PS	ZO	NS	NM	NB	NB	NB
PB	ZO	NS	NM	NB	NB	NB	NB

where α_e is the error of the direction, and $\dot{\alpha}_e$ is its change rate. The ranges of the above variables are given in Table I.

The domain of each antecedent and consequent is partitioned into seven overlapping triangular IT2 FSs (NB, NM, NS, ZO, PS, PM, and PB), as shown in Fig. 3. The rulebase is shown in Table II, which implements a usual diagonal controller similar to the fuzzy sliding mode controller [13], [32]. The minimum *t*-norm, and the Begian–Melek–Mendel type-reduction and defuzzification approach [2], [40], were used in the IT2 FLSs.

The overall IT2 FLS scheme is shown in Fig. 4.

IV. EXPERIMENTAL RESULTS

In this section, the performance of the proposed IT2 FLS is compared with that of a T1 FLS on a real MTWIP shown in Fig. 5. The two wheels, which are placed on the same axis, are directly connected to the output shaft of the DC-brushed motors. The configurations of the MTWIP are measured and given in Table III. However, no matter how carefully the parameters were measured, they cannot be 100% accurate, and hence there were inevitable modeling uncertainties due to inaccurately estimated parameters and external disturbances.

Fig. 6 shows the results from the first experiment, which involved only the balance controller. The initial condition was

TABLE III
VARIABLES AND THEIR CORRESPONDING UNCERTAINTIES OF THE MTWIP

Parameter	Value
$\hat{m}_w$ (kg)	0.14
$\hat{m}_b$ (kg)	2.58
$\hat{n}_{wa}$ (kg · m^2)	0.00014
$\hat{n}_{wd}$ (kg · m^2)	0.00054
$\hat{n}_{yb}$ (kg · m^2)	0.00128
$\hat{n}_{zb}$ (kg · m^2)	0.00128
$\hat{r}$ (m)	0.04
$\hat{b}$ (m)	0.15
$\hat{l}$ (m)	0.0622
$\hat{d}_b$	0.001
$\hat{d}_w$	0.01
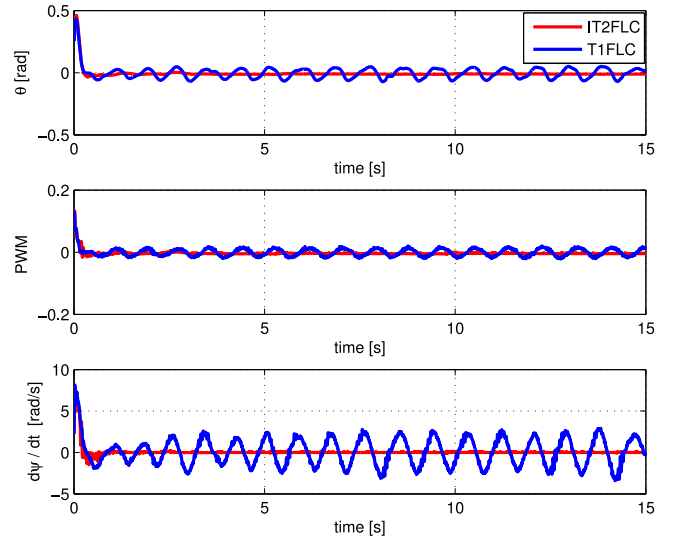
Fig. 6. Results from experiment 1: with the balance controller only.

$\mathbf{x}_0 = [0.48, 0, 0, 0]^T$. Observe that the T1 FLS resulted in persistent oscillations, whereas the IT2 FLS was very stable.

Fig. 7 shows the results from the second experiment, which tested the balance and position controllers together. The initial conditions were the same as those in Experiment 1, and the desired position was $p_d = 0.7$. Again, the T1 FLS resulted in persistent oscillations, but the IT2 FLS was very stable.

Fig. 8 shows the results from the third experiment, which included the balance, position, and direction controllers. The initial conditions were the same as those in the first two
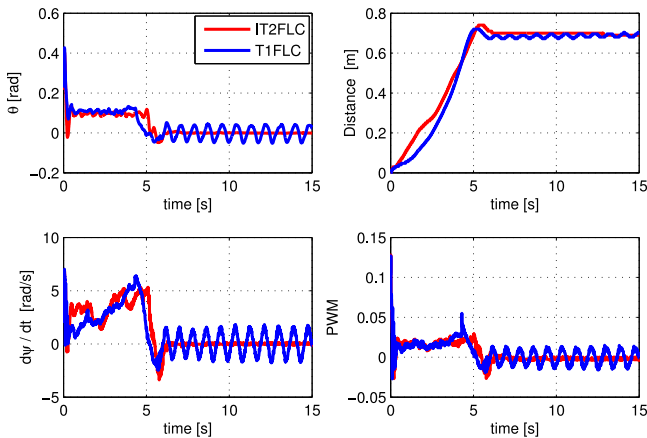
Fig. 7.   Results from experiment 2: with the balance and position controllers.
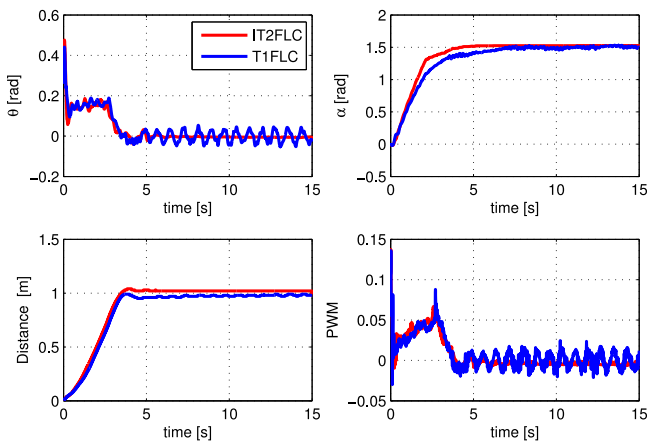
Fig. 8.   Results from experiment 3: with the balance, position, and direction controllers.

experiments. The desired position and direction were $p_d = 1$ and $\alpha_d = 1.5$. Fig. 9(a) and (b) show the sequential pictures taken from this experiment from two different angles. Observe that the T1 FLS resulted in persistent oscillations or steady-state errors, whereas the IT2 FLS was much more stable and accurate.

In summary, all three experiments showed that, when there were modeling uncertainties, the T1 FLS tended to produce persistent oscillations, whereas the IT2 FLS was much more stable and accurate. In other words, the IT2 FLS was better able to cope with modeling uncertainties.

V. Discussions

This section presents discussions on the robustness and stability of the proposed IT2 FLS.

A. Robustness of the IT2 FLS

In the previous section, we have shown, through real-world experiments, that the IT2 FLS was more robust than the T1 FLS. This conclusion is consistent with those in [19], [41]–[44].

But why IT2 FLSs are more robust? The reason was initially investigated in [45] and then in more details in [39]. We summarize their results here for the completeness of this paper.

Several researchers [19], [41], [43], [44] have shown that an IT2 FLS can give a smoother control surface than its T1 counterpart, especially in the region around the steady state [for a proportional-integral (PI) controller, this means that both the error and the change of error approach 0]. As a result, small disturbances around the steady state will not result in significant control signal changes and, thus, minimize the amount of oscillations. Wu and Tan [41], [44] made use of this property to design simplified IT2 FLSs, where IT2 FSs are only used for the region around 0 in each input domain, and T1 FSs are used in other regions. This simplified IT2 FLS preserves the robustness of traditional IT2 FLSs, with significantly reduced computational cost.

Wu and Tan [39], [45] then mathematically showed that when the baseline T1 FLS implements a linear PI controller and the IT2 FSs of the IT2 FLS are obtained from symmetrical perturbations of the T1 FSs, the resulting IT2 FLS implements a variable gain PI controller around the steady state. These gains are smaller than the original PI gains of the baseline T1 FLS, especially around the steady state. As a result, the IT2 FLS has a smoother control surface around the steady state. The PI gains of the IT2 FLS also change with the inputs, which cannot be achieved by the baseline T1 FLS.

However, all above analyses focused on IT2 FLSs using the Karnik–Mendel type-reducer. In this paper, we used the Nie–Tan and Begian–Melek–Mendel type-reducers for their simplicity. The robustness of IT2 FLSs using the Begian–Melek–Mendel type-reducer has been studied in [5]. It concluded that both T1 and IT2 FLSs can be designed to achieve robust behavior in various applications. However, IT2 FLSs have a more flexible structure and exhibited relatively small approximation errors in several examples in [5]. In this paper, we coupled several IT2 FLSs together, which makes a comprehensive robustness analysis more challenging. Nevertheless, this will be one of our future research directions.

B. Stability of the IT2 FLS

To facilitate the stability analysis of IT2 FLSs, Biglarbegian *et al.* [4] proposed an inference mechanism that was formulated in closed form and hence does not require the iterative Karnik–Mendel algorithms [27]. By using their inference mechanism, LMI stability conditions for IT2 TSK FLSs and IT2 TS FLSs were derived and transformed into the standard formats that can be easily solved using software tools such as the MATLAB LMI toolbox. Furthermore, Jafarzadeh *et al.* [17], [18] obtained stability conditions for general type-2 TSK FLSs. Unlike results using a common Lyapunov function, their results do not require the stability of all consequents for stability investigation.

In this paper, we proved the stability of IT2 TS FLSs in a different way. By using the Nie–Tan method, the defuzzified output of the IT2 FLS can be described by (4), which has the same structure as the T1 FLS studied in [16], [35]. Therefore,
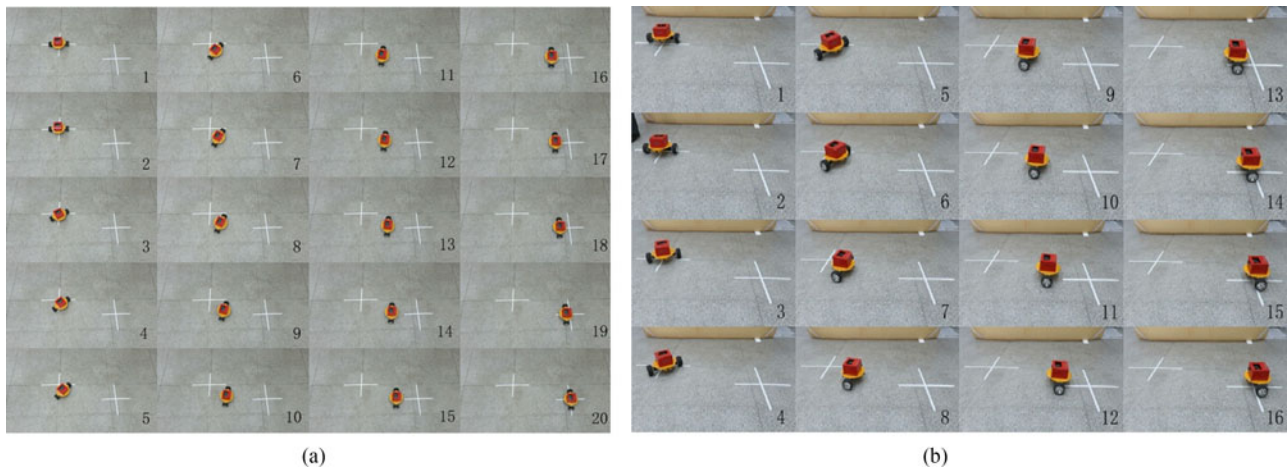
Fig. 9.   Experiment pictures taken from (a) the top and (b) the side of the MTWIP.

the related stability conditions of T1 FLS can be easily applied in our IT2 FLS case.

VI. CONCLUSION

In this paper, an integrated IT2 FLS that simultaneously models and controls an MTWIP was proposed, and its effectiveness was verified through real-world experiments. Our results showed that the designed IT2 FLS was better able to cope with the modeling uncertainties than its T1 counterpart and performed better on the actual plant. These results are consistent with previous findings in the literature [19], [41]–[44].

REFERENCES

[1] D. Anderson, *nBot balancing robot*. 2013. [Online]. Available: http://www.geology.smu.edu/˜dpa-www/robo/nbot/. Accessed on: Jan. 11, 2016.

[2] M. Begian, W. Melek, and J. Mendel, "Stability analysis of type-2 fuzzy systems," in *Proc. IEEE Int Conf. Fuzzy Syst.*, Hong Kong, Jun. 2008, pp. 947–953.

[3] P. Benjamas and C. Phichitphon, "Self-balancing iBOT-like wheelchair based on type-1 and interval type-2 fuzzy control," in *Proc. 11th Int. Conf. Elect. Eng./Electron. Comput. Telecommun. Inf. Technol.*, Nakhon Ratchasima, Thailand, May 2014, pp. 1–6.

[4] M. Biglarbegian, W. Melek, and J. Mendel, "On the stability of interval type-2 TSK fuzzy logic control systems," *IEEE Trans. Syst. Man Cybern.–B*, vol. 41, no. 5, pp. 798–818, Jun. 2010.

[5] M. Biglarbegian, W. Melek, and J. Mendel, "On the robustness of type-1 and interval type-2 fuzzy logic systems in modeling," *Inf. Sci.*, vol. 181, no. 7, pp. 1325–1347, 2011.

[6] O. Castillo and P. Melin, *Type-2 Fuzzy Logic Theory and Applications*. Berlin, Germany: Springer-Verlag, 2008.

[7] L. Cervantes and O. Castillo, "Type-2 fuzzy logic aggregation of multiple fuzzy controllers for airplane flight control," *Inf. Sci.*, vol. 324, pp. 247–256, 2015.

[8] C. Chiu, "The design and implementation of a wheeled inverted pendulum using an adaptive output recurrent cerebellar model articulation controller," *IEEE Trans. Ind. Electron.*, vol. 57, no. 5, pp. 1814–1822, May 2010.

[9] F. Dai, X. Gao, and S. Jiang, "A two-wheeled inverted pendulum robot with friction compensation," *Mechatronics*, vol. 30, pp. 116–125, 2015.

[10] F. Grasser, A. D'Arrigo, S. Colombi, and A. Rufer, "Joe: A mobile, inverted pendulum," *IEEE Trans. Ind. Electron.*, vol. 49, no. 1, pp. 107–114, Feb. 2002.

[11] Y. Ha and S. Yuta, "Trajectory tracking control for navigation of the inverse pendulum type self-contained mobile robot," *Robot. Auton. Syst.*, vol. 17, no. 1/2, pp. 65–80, 1996.

[12] H. Hagras, "Type-2 FLCs: A new generation of fuzzy controllers," *IEEE Comput. Intell. Mag.*, vol. 2, no. 1, pp. 30–43, Feb. 2007.

[13] H. Hellendoorn and R. Palm, "Fuzzy system technologies at Siemens R&D," *Fuzzy Sets Syst.*, vol. 63, no. 3, pp. 245–269, 1994. [Online]. Available: http://www.sciencedirect.com/science/article/pii/0165011494902143

[14] C. Huang, W. Wang, and C. Chiu, "Design and implementation of fuzzy control on a two-wheel inverted pendulum," *IEEE Trans. Ind. Electron.*, vol. 58, no. 7, pp. 2988–3001, Jul. 2011.

[15] J. Huang, T. Fukuda, and T. Matsuno, "Modeling and velocity control for a novel narrow vehicle based on mobile wheeled inverted pendulum," *IEEE Trans. Control Syst. Technol.*, vol. 21, no. 5, pp. 1607–1617, Sep. 2013.

[16] J. Huang, S. Ri, L. Liu, Y. Wang, J. Kim, and G. Pak, "Nonlinear disturbance observer-based dynamic surface control of mobile wheeled inverted pendulum," *IEEE Trans. Control Syst. Technol.*, vol. 23, no. 6, pp. 2400–2407, Nov. 2015.

[17] S. Jafarzadeh, S. Fadali, and A. Sonbol, "Stability analysis and control of discrete type-1 and type-2 TSK fuzzy systems: Part I stability analysis," *IEEE Trans. Fuzzy Syst.*, vol. 19, no. 6, pp. 989–1000, Dec. 2011.

[18] S. Jafarzadeh, S. Fadali, and A. Sonbol, "Stability analysis and control of discrete type-1 and type-2 TSK fuzzy systems: Part II control design," *IEEE Trans. Fuzzy Syst.*, vol. 19, no. 6, pp. 1001–1013, Dec. 2011.

[19] E. A. Jammeh, M. Fleury, C. Wagner, H. Hagras, and M. Ghanbari, "Interval type-2 fuzzy logic congestion control for video streaming across IP networks," *IEEE Trans. Fuzzy Syst.*, vol. 17, no. 5, pp. 1123–1142, Oct. 2009.

[20] E. Kim and H. Lee, "New approaches to relaxed quadratic stability condition of fuzzy control systems," *IEEE Trans. Fuzzy Syst.*, vol. 8, no. 5, pp. 523–534, Oct. 2000.

[21] H. Lee and S. Jung, "Balancing and navigation control of a mobile inverted pendulum robot using sensor fusion of low cost sensors," *Mechatronics*, vol. 22, no. 1, pp. 95–105, 2012.

[22] Z. Li and J. Luo, "Adaptive robust dynamic balance and motion controls of mobile wheeled inverted pendulums," *IEEE Trans. Control Syst. Technol.*, vol. 17, no. 1, pp. 233–241, Jan. 2009.

[23] Q. Liang, N. N. Karnik, and J. M. Mendel, "Connection admission control in ATM networks using survey-based type-2 fuzzy logic systems," *IEEE Trans. Syst. Man Cybern.*, vol. 30, no. 3, pp. 329–339, Aug. 2000.

[24] Q. Liang and J. M. Mendel, "Equalization of nonlinear time-varying channels using type-2 fuzzy adaptive filters," *IEEE Trans. Fuzzy Syst.*, vol. 8, no. 5, pp. 551–563, Oct. 2000.

[25] P. Melin, L. Astudillo, O. Castillo, F. Valdez, and M. Garcia, "Optimal design of type-2 and type-1 fuzzy tracking controllers for autonomous mobile robots under perturbed torques using a new chemical optimization paradigm," *Expert Syst. Appl.*, vol. 40, no. 8, pp. 3185–3195, 2013.

[26] P. Melin, O. Mendoza, and O. Castillo, "Face recognition with an improved interval type-2 fuzzy logic Sugeno integral and modular neural networks," *IEEE Trans Syst. Man Cybern., A*, vol. 41, no. 5, pp. 1001–1012, Sep. 2011.

[27] J. M. Mendel, *Uncertain Rule-Based Fuzzy Logic Systems: Introduction and New Directions*. Upper Saddle River, NJ, USA: Prentice-Hall, 2001.

[28] J. M. Mendel, R. I. John, and F. Liu, "Interval type-2 fuzzy logic systems made simple," *IEEE Trans. Fuzzy Syst.*, vol. 14, no. 6, pp. 808–821, Dec. 2006.

[29] E. Mohammad and M. Ahmad, "Interval type-2 fuzzy PID controller for uncertain nonlinear inverted pendulum system," *ISA Trans.*, vol. 53, pp. 732–743, 2014.

[30] M. Muhammad, S. Buyamin, M. Ahmad, and S. Nawawi, "Takagi-Sugeno fuzzy modeling of a two-wheeled inverted pendulum robot," *J. Intell. Fuzzy Syst.*, vol. 25, pp. 535–546, 2013.

[31] M. Nie and W. W. Tan, "Towards an efficient type-reduction method for interval type-2 fuzzy logic systems," in *Proc. IEEE Int. Conf. Fuzzy Syst.*, Hong Kong, Jun. 2008, pp. 1425–1432.

[32] R. Palm, "Sliding mode fuzzy control," in *Proc. IEEE Int. Conf. Fuzzy Syst.*, San Diego, CA, USA, March 1992, pp. 519–526.

[33] K. Pathak, J. Franch, and S. Agrawal, "Velocity and position control of a wheeled inverted pendulum by partial feedback linearization," *IEEE Trans. Robot.*, vol. 21, no. 3, pp. 505–513, Jun. 2005.

[34] S. Ri, J. Huang, Y. Wang, M. Kim, and S. An, "Terminal sliding mode control of mobile wheeled inverted pendulum system with nonlinear disturbance observer," *Math. Probl. Eng.*, vol. 2014, 2014, Art. no. 284216.

[35] A. Salerno and J. Angeles, "A new family of two-wheeled mobile robots: Modeling and controllability," *IEEE Trans. Robot.*, vol. 23, no. 1, pp. 169–173, Feb. 2007.

[36] M. A. Sanchez, O. Castillo, and J. R. Castro, "Generalized type-2 fuzzy systems for controlling a mobile robot and a performance comparison with interval type-2 and type-1 fuzzy systems," *Expert Syst. Appl.*, vol. 42, no. 14, pp. 5904–5914, 2015.

[37] K. Tai, A.-R. El-Sayed, M. Biglarbegian, C. I. Gonzalez, O. Castillo, and S. Mahmud, "Review of recent type-2 fuzzy controller applications," *Algorithms*, vol. 9, no. 2, p. 39, 2016.

[38] C. Tseng, B. Chen, and H. Uang, "Fuzzy tracking control design for nonlinear dynamic systems via T-S fuzzy model," *IEEE Trans. Fuzzy Syst.*, vol. 9, no. 3, pp. 381–392, Jun. 2001.

[39] D. Wu, "On the fundamental differences between interval type-2 and type-1 fuzzy logic controllers," *IEEE Trans. Fuzzy Syst.*, vol. 20, no. 5, pp. 832–848, Oct. 2012.

[40] D. Wu, "Approaches for reducing the computational cost of interval type-2 fuzzy logic systems: Overview and comparisons," *IEEE Trans. Fuzzy Syst.*, vol. 21, no. 1, pp. 80–99, Feb. 2013.

[41] D. Wu and W. W. Tan, "A simplified architecture for type-2 FLSs and its application to nonlinear control," in *Proc. IEEE Conf. Cybern. Intell. Syst.*, Singapore, Dec. 2004, pp. 485–490.

[42] D. Wu and W. W. Tan, "A type-2 fuzzy logic controller for the liquid-level process," in *Proc. IEEE Int. Conf. Fuzzy Syst.*, Budapest, Hungary, Jul. 2004, vol. 2, pp. 953–958.

[43] D. Wu and W. W. Tan, "Genetic learning and performance evaluation of type-2 fuzzy logic controllers," *Eng. Appl. Artif. Intell.*, vol. 19, no. 8, pp. 829–841, 2006.

[44] D. Wu and W. W. Tan, "A simplified type-2 fuzzy controller for real-time control," *ISA Trans.*, vol. 15, no. 4, pp. 503–516, 2006.

[45] D. Wu and W. W. Tan, "Interval type-2 fuzzy PI controllers: Why they are more robust," in *Proc. IEEE Int. Conf. Granular Comput.*, San Jose, CA, USA, Aug. 2010, pp. 802–807.

[46] J. Xu, Z. Guo, and T. Lee, "Design and implementation of a Takagi-Sugeno-type fuzzy logic controller on a two-wheeled mobile robot," *IEEE Trans. Ind. Electron.*, vol. 60, no. 12, pp. 5717–5728, Dec. 2013.

Authors' photographs and biographies not available at the time of publication.